



Pulmonary metastases from malignant epithelioid schwannoma of the arm presenting as fast-growing subsolid nodules: Report of an unusual case

Andrea Borghesi^{a,*}, Luisa Bercich^b, Silvia Michelini^c, Francesco Bertagna^d, Alessandra Scrimieri^a, Roberto Maroldi^a

^a Department of Radiology, University and ASST Spedali Civili of Brescia, Brescia, Italy

^b Department of Pathology, ASST Spedali Civili of Brescia, Brescia, Italy

^c Department of Radiology, Fondazione Poliambulanza Istituto Ospedaliero, Brescia, Italy

^d Nuclear Medicine, University and ASST Spedali Civili of Brescia, Brescia, Italy

ARTICLE INFO

Keywords:

Soft tissue neoplasm
Malignant epithelioid schwannoma
Pulmonary metastases
Subsolid nodule
Multidetector-row computed tomography
Follow-up studies

ABSTRACT

Subsolid pulmonary nodules (SSNs) may be the manifestation of benign and malignant conditions. Malignant SSNs usually correspond to the preinvasive or invasive lepidic growth of pulmonary adenocarcinomas. More rarely, malignant SSNs may be the manifestation of primitive pulmonary lymphomas or metastases from extrapulmonary malignancies. In the case of metastases from extrapulmonary malignancies, the SSNs exhibit more aggressive behavior with rapid growth in a short period of time. The present article describes the first case of pulmonary metastases presenting as fast-growing SSNs in a patient with malignant epithelioid schwannoma of the arm.

1. Introduction

Subsolid pulmonary nodules (SSNs) manifest on thin-section multidetector computed tomography (MDCT) as part solid or pure ground-glass nodules, depending on the presence or absence of a solid component within the lesion [1–3]. SSNs may be the manifestation of benign and malignant conditions. Malignant SSNs usually correspond to the preinvasive or invasive lepidic growth of pulmonary adenocarcinomas [1–3]. This type of lesion may remain stable for years or show heterogeneous growth patterns with a trend toward a progressive increase in size over time [1–3]. More rarely, malignant SSNs may be the manifestation of primitive pulmonary lymphomas [4] or metastases from extrapulmonary malignancies, most often from malignant melanoma [5–9].

Pulmonary metastases presenting as SSNs exhibited more aggressive behavior with rapid growth in a short period of time [5–8].

Malignant epithelioid schwannoma is a rare neoplasm derived from

the neural crest with features of Schwann cell differentiation [10]. This tumor may occur at any age but is most common between the third and the fourth decades of life and occurs more frequently in women than in men. The extremities are the most common sites, and the growths are typically located in deep soft tissue. Immunohistochemically, the tumor cells show strong and diffuse staining for the S-100 protein with no expression of melanocytic markers and cytokeratin [10,11]. INI1 immunostaining may also be useful in the diagnosis of malignant epithelioid schwannoma; however, the literature reports that the loss of INI1 expression in this tumor ranges from 27 to 67% [12–14]. Therefore, the diagnostic contribution of INI1 is mainly observed when there are problems in differentiating malignant epithelioid schwannoma from melanoma [12,14].

The prognosis of these tumors is poor due to their aggressive behavior and their high metastatic potential [10].

The present article describes the first case of pulmonary metastases presenting as fast-growing SSNs in a patient with malignant epithelioid

* Corresponding author at: Department of Radiology, University and Spedali Civili of Brescia, Piazzale Spedali Civili, 1, I – 25123, Brescia, Italy.
E-mail address: andrea.borghesi@unibs.it (A. Borghesi).

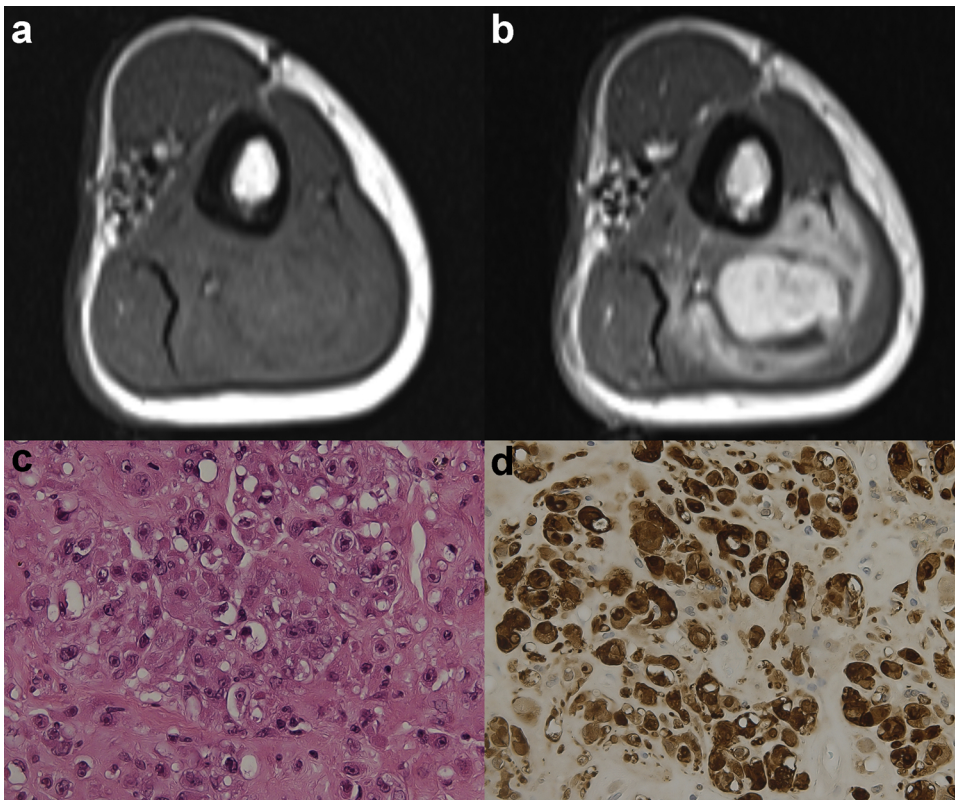


Fig. 1. Axial T1-weighted sequences of the left arm before (a) and after (b) gadolinium contrast medium administration that show the intense and heterogeneous enhancement of the mass. Note the absence of the split fat sign. (c) Image of histological hematoxylin and eosin staining of the lesion at 40x, showing the epithelioid cells with abundant eosinophilic cytoplasm and prominent nucleoli. (d) The tumor cells display diffuse and strong S100 protein positivity.

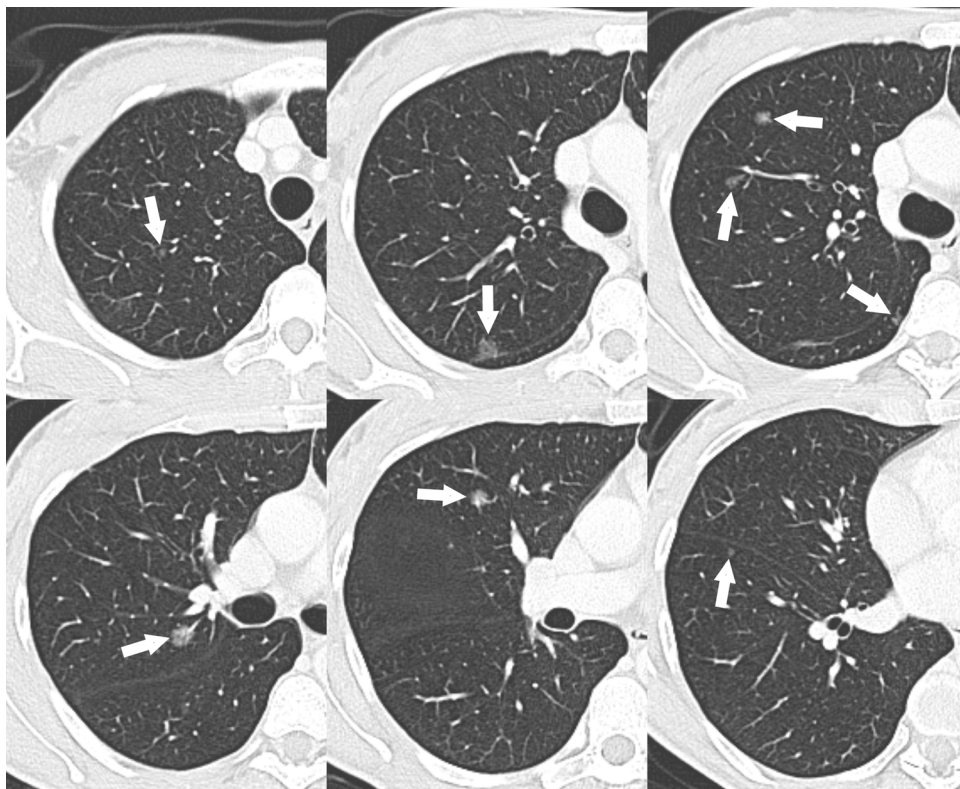


Fig. 2. Cropped axial CT images with lung window setting showing the SSNs in the right lung (arrows).

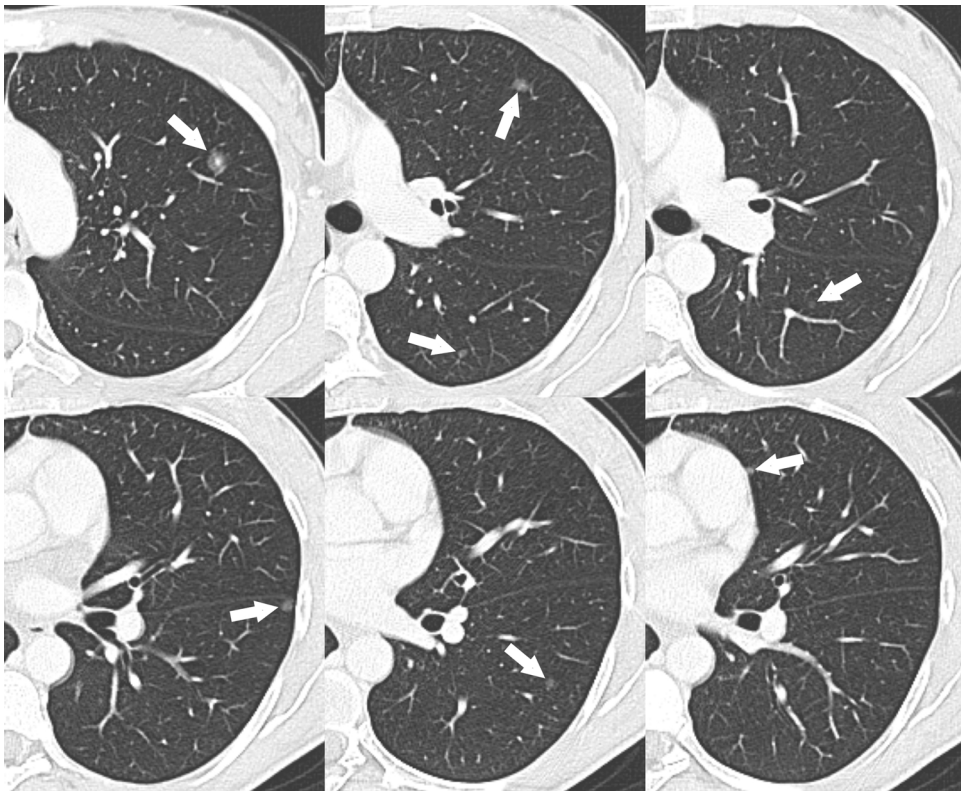


Fig. 3. Cropped axial CT images with lung window setting showing the SSNs in the left lung (arrows).

schwannoma of the left arm.

2. Case report

A 43-year-old white European female was referred to our radiology department to undergo an MRI for the evaluation of a growing mass in the left arm. The patient's medical history was unremarkable, and there was no evidence of systemic disease or hereditary syndromes.

Magnetic resonance imaging (MRI) showed a 5 x 4 cm mass arising from the subfascial soft tissue of the posterior compartment of the left arm (Fig. 1a, and b). On contrast-enhanced T1-weighted sequence, the mass exhibited intense and heterogeneous enhancement (Fig. 1b). No rim of fat around the mass (split-fat sign) was detectable (Fig. 1a).

In view of the characteristics of the lesion, which were suggestive of a malignant neoplasm of the soft tissue, a fine needle aspiration biopsy was performed.

The histologic examination of the biopsy revealed neoplastic proliferation with epithelioid morphology (Fig. 1c), 10 mitosis/10 HPF and a MIB1/Ki67 proliferative index of 20%. The epithelioid cells exhibited an abundant eosinophilic cytoplasm with prominent nucleoli (Fig. 1c). On immunohistochemical analysis, the epithelioid cells showed strong and diffuse positivity for the S-100 protein (Fig. 1d). Staining for HMB45, MART1, MITF, tyrosinase, cytokeratins, VIII factor, and CD31 were negative.

Based on the morphological features, the immunophenotype, the mitosis and the proliferative index, a diagnosis of malignant epithelioid schwannoma was made.

Thus, a total-body computed tomography (CT) scan with and

without contrast was performed. The CT scan revealed multiple pulmonary lesions with the appearance of SSNs (Figs. 2, and 3). The total number of pulmonary nodules detected by CT scan was 15 (8 in the right lung and 7 in the left lung) and their diameters ranged from 4 to 11 mm (Figs. 2, and 3). No other lesions were found in the rest of the body; in particular, non-pathological hilar or mediastinal lymph nodes were observed.

Our provisional diagnosis was atypical presentation of pulmonary metastases from malignant epithelioid schwannoma. However, the hypothesis of multifocal preinvasive/minimally invasive pulmonary adenocarcinoma was also considered.

The soft tissue mass was surgically removed with radial nerve sparing. The surgical margin was marginal; therefore, the patient underwent local radiotherapy and adjuvant chemotherapy.

With regard for the pulmonary lesions, the number (15), the size (4–11 mm) and the CT attenuation (subsolid) of the nodules would have made pulmonary resections very complex and risky. In addition, the aggressiveness of the epithelioid malignant schwannoma, its high metastatic potential and the surgical margin of the soft tissue mass were also considered. For these reasons, lung surgery was not considered a viable therapeutic option.

The first follow-up chest CT scan, performed 4 months from baseline, showed a significant reduction in the size and density of the SSNs (Fig. 4). The reduction in size and density of the nodules during chemotherapy treatment further strengthened the diagnosis of pulmonary metastases.

A positron emission tomography (PET)/CT scan, obtained 9 months from baseline, revealed the 18-fluorodeoxyglucose (^{18}F FDG) uptake of

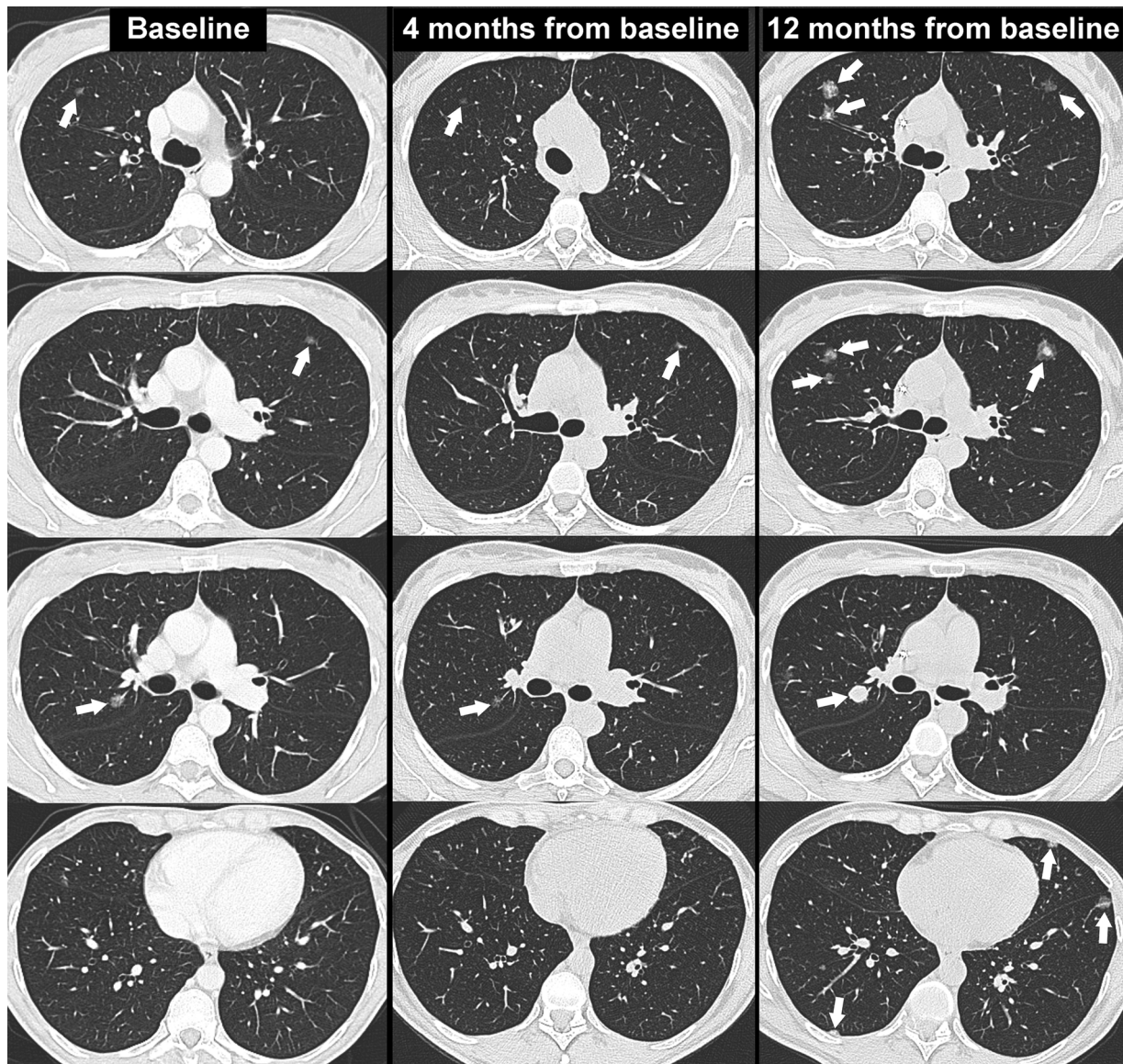


Fig. 4. Series of axial CT images with lung window setting at the baseline (column on the left), at the first follow-up (column in the center) and at 12 months from the baseline (column on the right) that show the changes in the size, density and number of SSNs during the follow-up (arrows).

the pulmonary nodules (Fig. 5). Pathological ^{18}F FDG uptake was also observed in the left axillary lymph nodes, at the level of the vertebral body of C3, the right pedicle of T10, the right femur and the left iliac crest (Fig. 5).

The next CT follow-up scan, performed 12 months from baseline (during chemotherapy treatment), showed disease progression, with a significant increase in the size, density and number of SSNs (Fig. 4). In subsequent imaging follow-ups, the disease progressed further, despite chemotherapy treatment (Fig. 6). The patient died of respiratory failure 21 months after diagnosis.

3. Discussion

SSNs pose a complex diagnostic challenge, as they may be the

manifestation of different diseases, both benign and malignant, such as inflammation, focal interstitial fibrosis, primary neoplasm and metastases. In contrast to benign lesions, malignancies persist and tend to have different growth patterns [1–3]. Primary pulmonary tumors presenting as SSNs on thin-section MDCT are typically lepidic growth adenocarcinoma [2–3]. These lesions often exhibit an indolent course with very slow growth rates [2–3,15–18].

Pulmonary metastases presenting as SSNs are unusual [19] and typically exhibit a fast growth rate, with a doubling time ≤ 230 days [5–7].

In a literature search of the PubMed database for publications from the past 15 years using the key words metastasis/metastatic and SSN/ground-glass nodule, we identified eight English-language case reports in which pulmonary metastases presenting as SSNs were described

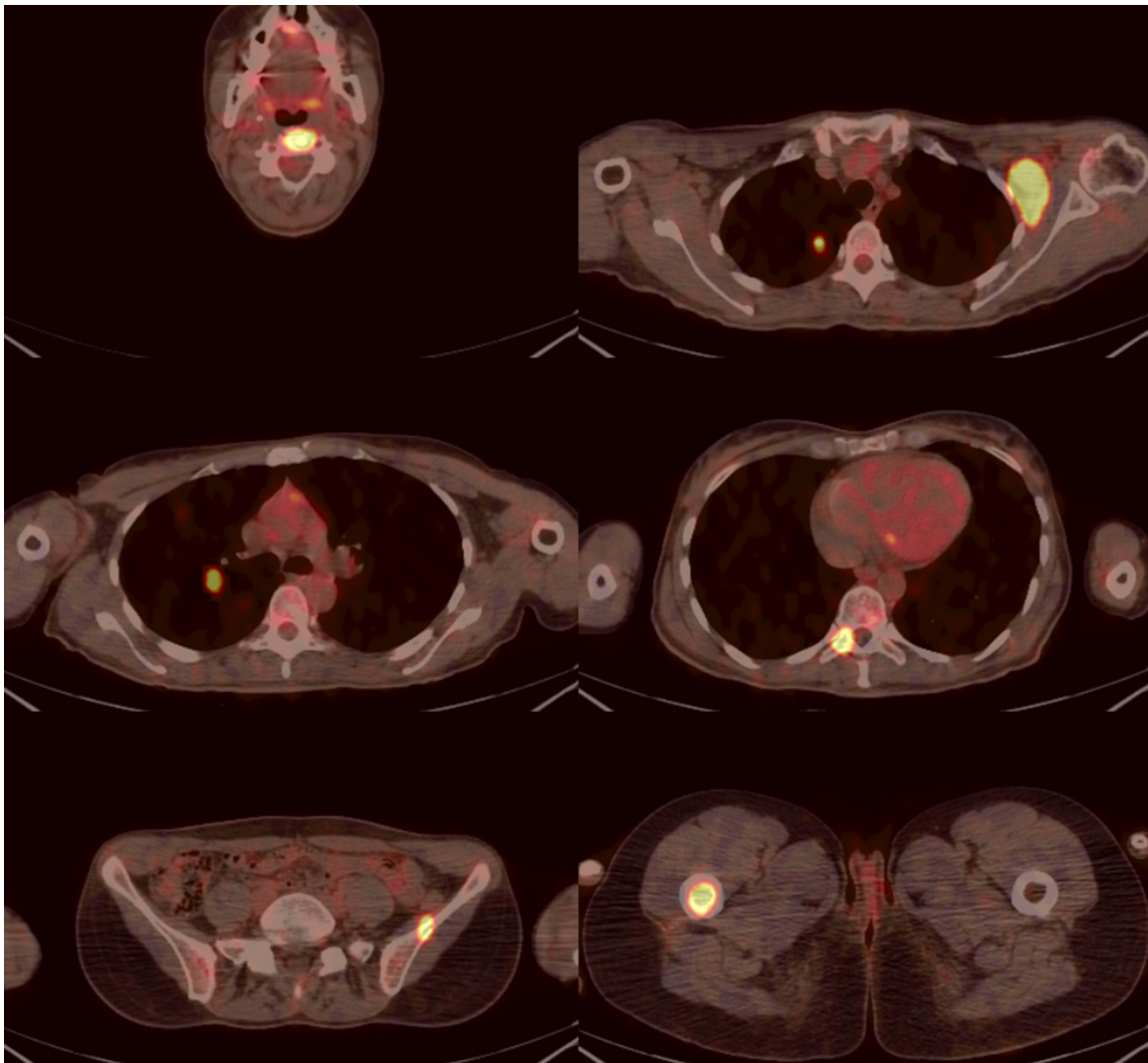


Fig. 5. Series of axial PET/CT images showing the pathological ^{18}F FDG uptake within the lungs, left axilla and bones (vertebral body of C3, right pedicle of T10, right femur and left iliac crest).

(Table 1) [5–9,20–22].

Based on these published data and previous articles, the SSN appearance of pulmonary metastases is most frequently observed in patients with malignant melanoma [5–9]. Infrequently, this presentation pattern may be observed in pulmonary metastases from spindle cell carcinoma of the kidney [20], cholangiocarcinoma [21], prostate cancer [22], choriocarcinoma and angiosarcoma [23]. While in choriocarcinoma and angiosarcoma SSN appearance is due to the fragility of the metastatic neovascular tissue [23], the SSN appearance of the pulmonary metastases from melanoma, spindle cell carcinoma, cholangiocarcinoma and prostate cancer reflects the partial effacement of the alveolar architecture by the neoplastic tissue [5–9,20–22].

To the best of our knowledge, the present article describes the first reported case of pulmonary metastases presenting as SSNs from malignant epithelioid schwannoma. Although in our case there was no histological examination, the diagnosis of pulmonary metastases

was confirmed by the behavior of the SSNs during follow-up (i.e., significant reduction in size and density after the first cycles of chemotherapy and then rapid progression of the pulmonary disease with development of metastases in other sites). In our case, the SSN appearance of pulmonary metastases was probably similar to that recently reported in the pulmonary metastases from melanoma [9]. This statement is supported by the progressive increase in the density of the pulmonary metastases from pure nodules to part solid/solid nodules (Fig. 7), which reflected the progressive effacement of the alveolar architecture.

Similar to what has been reported in the literature [5–8], the SSNs detected in the present case exhibited fast growth rates (Figs. 4, 6, and 7).

In the present case, pulmonary metastases also showed pathological ^{18}F FDG uptake on PET/CT imaging that indicated their hypermetabolic activity. However, the role of ^{18}F FDG PET/CT in the differential diagnosis of primitive and metastatic SSNs is not well understood [8,24]. In



Fig. 6. Chest X-ray, performed 19 months after baseline, showing the significant progression of the pulmonary metastases. Bilateral pleural effusion is also shown.

Table 1
Pulmonary metastases presenting as SSNs reported in the literature (last 15 years).

Authors	Year	Number of SSNs	Primary cancer
Okita R et al [5]	2005	Multiple	Melanoma
Yanagawa et al [20]	2006	Single	Spindle cell carcinoma (<i>kidney</i>)
Kang MJ et al [6]	2010	Single	Melanoma
Mizuuchi H et al [7]	2015	Single	Melanoma (<i>bulbar conjunctiva</i>)
Dal Piaz G et al [8]	2018	Single	Melanoma
Sakamoto et al [21]	2018	Single	Cholangiocarcinoma
Lubin DJ et al [22]	2019	Single	Prostate
Borghesi A et al [9]	2019	Single*	Melanoma
Present case	2019	Multiple	Malignant epithelioid schwannoma (<i>soft tissue of the arm</i>)

* In this case report, the patient exhibited two pulmonary metastases (one subsolid and the other solid). SSNs, subsolid nodules.

the future, a possible solution to this problem could be to use PET/CT-specific tracers for the different cancer histotypes [22].

4. Conclusion

The present article describes the first reported case in the literature involving the occurrence of pulmonary metastases with SSN appearance in a patient with malignant epithelioid schwannoma. Because the

appearance of metastatic SSNs on baseline CT is similar to that of primitive lesions, the presence of SSNs with a rapid growth in a patient with a previous cancer history should increase the suspicion of metastatic disease, especially if there are multiple lesions and the lesions are positive on ^{18}F FDG PET/CT imaging.

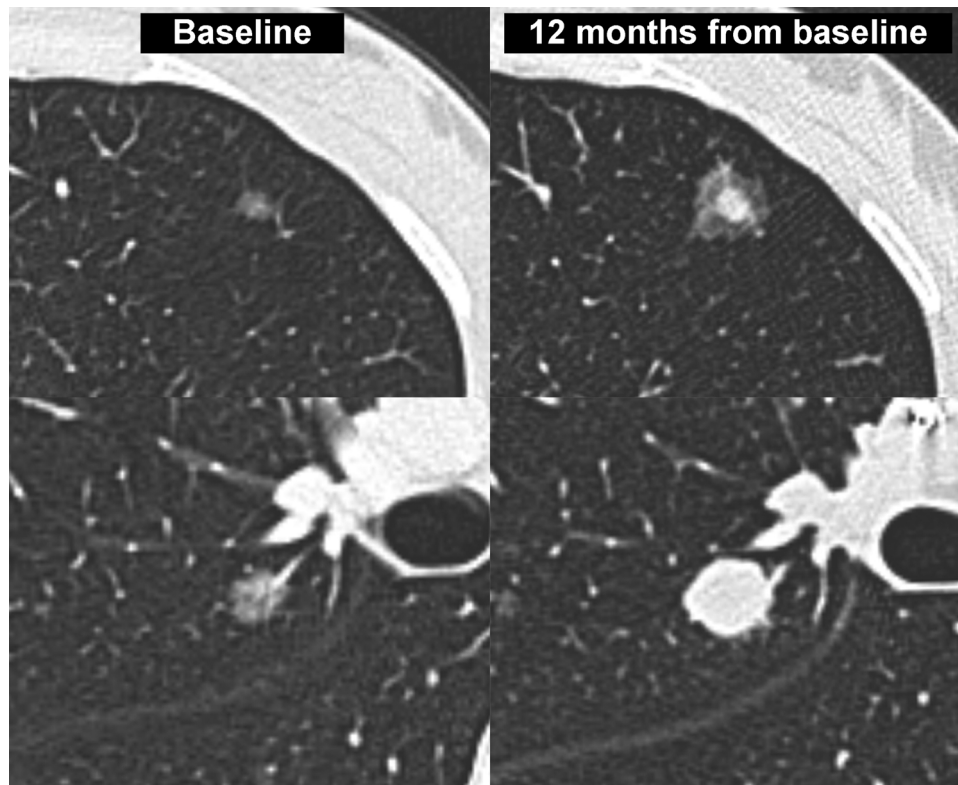


Fig. 7. Cropped axial CT images at the baseline (column on the left) and at 12 months from baseline (column on the right) showing the change in size and density of two pulmonary metastases. From pure to part solid nodule at the top and from pure to solid nodule at the bottom.

Declaration of Competing Interest

The authors declare no financial or other conflict of interest

References

- [1] A. Borghesi, S. Michelini, F. Bertagna, A. Scrimieri, S. Pezzotti, R. Maroldi, Hilly or mountainous surface: a new CT feature to predict the behavior of pure ground glass nodules? *Eur. J. Radiol. Open* 5 (2018) 177–182, <https://doi.org/10.1016/j.ejro.2018.09.004>.
- [2] A. Borghesi, D. Farina, S. Michelini, M. Ferrari, D. Benetti, S. Fisogni, A. Tironi, R. Maroldi, Pulmonary adenocarcinomas presenting as ground-glass opacities on multidetector CT: three-dimensional computer-assisted analysis of growth pattern and doubling time, *Diagn. Interv. Radiol.* 22 (2016) 525–533, <https://doi.org/10.5152/dir.2016.16110>.
- [3] A. Borghesi, A. Scrimieri, S. Michelini, G. Calandra, S. Golemi, A. Tironi, R. Maroldi, Quantitative CT analysis for predicting the behavior of part-solid nodules with solid components less than 6 mm: size, density and shape descriptors, *Appl. Sci.* 9 (2019) 3428.
- [4] D. Albano, A. Borghesi, G. Bosio, M. Bertoli, R. Maroldi, R. Giubbini, F. Bertagna, Pulmonary mucosa-associated lymphoid tissue lymphoma: ^{18}F -FDG PET/CT and CT findings in 28 patients, *Br. J. Radiol.* 90 (2017), <https://doi.org/10.1259/bjr.20170311>.
- [5] R. Okita, M. Yamashita, M. Nakata, N. Teramoto, A. Bessho, H. Mogami, Multiple ground-glass opacity in metastasis of malignant melanoma diagnosed by lung biopsy, *Ann. Thorac. Surg.* 79 (2005) e1–2.
- [6] M.J. Kang, M.A. Kim, C.M. Park, C.H. Lee, J.M. Goo, H.J. Lee, Ground-glass nodules found in two patients with malignant melanomas: different growth rate and different histology, *Clin. Imaging* 34 (2010) 396–399, <https://doi.org/10.1016/j.clinimag.2009.10.036>.
- [7] H. Mizuuchi, K. Suda, H. Kitahara, S. Shimamatsu, M. Kohno, T. Okamoto, Y. Maehara, Solitary pulmonary metastasis from malignant melanoma of the bulbar conjunctiva presenting as a pulmonary ground glass nodule: report of a case, *Thorac. Cancer* 6 (2015) 97–100, <https://doi.org/10.1111/1759-7714.12124>.
- [8] G. Dalpiaz, S. Asioli, S. Fanti, G. Rea, E. Marchiori, Rapidly growing pulmonary ground-glass nodule caused by metastatic melanoma lacking uptake on ^{18}F -FDG PET-CT, *J. Bras. Pneumol.* 44 (2018) 171–172.
- [9] A. Borghesi, A. Tironi, S. Michelini, A. Scrimieri, D. Benetti, R. Maroldi, Two synchronous lung metastases from malignant melanoma: the same patient but different morphological patterns, *Eur. J. Radiol. Open* 6 (2019) 287–290, <https://doi.org/10.1016/j.ejro.2019.08.001>.
- [10] P. Lodding, L.G. Kindblom, L. Angervall, Epithelioid malignant schwannoma. A study of 14 cases, *Virchows Arch. A Pathol. Anat. Histopathol.* 409 (1986) 433–451.
- [11] W.B. Laskin, S.W. Weiss, G.L. Brattbauer, Epithelioid variant of malignant peripheral nerve sheath tumor (malignant epithelioid schwannoma), *Am. J. Surg. Pathol.* 15 (1991) 1136–1145.
- [12] J.L. Hornick, P. Dal Cin, C.D. Fletcher, Loss of INI1 expression is characteristic of both conventional and proximal type epithelioid sarcoma, *Am. J. Surg. Pathol.* 33 (2009) 542–550, <https://doi.org/10.1097/PAS.0b013e3181882c54>.
- [13] V.Y. Jo, C.D. Fletcher, Epithelioid malignant peripheral nerve sheath tumor: clinicopathologic analysis of 63 cases, *Am. J. Surg. Pathol.* 39 (2015) 673–682, <https://doi.org/10.1097/PAS.0000000000000379>.
- [14] B. Rekhi, K. Kosemehmetoglu, G.G. Tezel, S. Dervisoglu, Clinicopathologic features and immunohistochemical spectrum of 11 cases of epithelioid malignant peripheral nerve sheath tumors, including INI1/SMARCB1 results and BRAF V600E analysis, *APMIS* 125 (2017) 679–689, <https://doi.org/10.1111/apm.12702>.
- [15] M.C. Godoy, D.P. Naidich, Subsolid pulmonary nodules and the spectrum of peripheral adenocarcinomas of the lung: recommended interim guidelines for assessment and management, *Radiology* 253 (2009) 606–622, <https://doi.org/10.1148/radiol.2533090179>.
- [16] M.C. Godoy, B. Sabloff, D.P. Naidich, Subsolid pulmonary nodules: imaging evaluation and strategic management, *Curr. Opin. Pulm. Med.* 18 (2012) 304–312.
- [17] H. MacMahon, D.P. Naidich, J.M. Goo, K.S. Lee, A.N.C. Leung, J.R. Mayo, A.C. Mehta, Y. Ohno, C.A. Powell, M. Prokop, G.D. Rubin, C.M. Schaefer-Prokop, W.D. Travis, P.E. Van Schil, A.A. Bankier, Guidelines for Management of Incidental Pulmonary Nodules Detected on CT Images: From the Fleischner Society 2017, *Radiology* 284 (2017) 228–243, <https://doi.org/10.1148/radiol.2017161659>.
- [18] R. Yip, D.F. Yankelevitz, M. Hu, K. Li, D.M. Xu, A. Jirapatnakul, C.I. Henschke, Lung Cancer deaths in the national lung screening trial attributed to nonsolid nodules, *Radiology* 281 (2016) 589–596.
- [19] C.M. Park, J.M. Goo, T.J. Kim, H.J. Lee, K.W. Lee, C.H. Lee, Y.T. Kim, K.G. Kim, H.Y. Lee, E.A. Park, J.G. Im, Pulmonary nodular ground-glass opacities in patients with extrapulmonary cancers: what is their clinical significance and how can we determine whether they are malignant or benign lesions? *Chest* 133 (2008) 1402–1409, <https://doi.org/10.1378/chest.07-2568>.
- [20] M. Yanagawa, K. Kuriyama, M. Koyama, M. Higashiyama, Y. Tsukamoto, J. Arisawa, N. Tomiyama, H. Nakamura, Solitary pulmonary metastases from renal cell carcinoma: comparison of high resolution CT with pathological findings,

- Radiat. Med. 24 (2006) 680–686.
- [21] T. Sakamoto, S. Honjo, M. Morimoto, M. Amisaki, Y. Arai, N. Tokuyasu, K. Ashida, H. Saito, K. Nosaka, Y. Fujiwara, Successful resection of a slow-growing synchronous pulmonary metastasis from distal cholangiocarcinoma resected 3.5 years after initial surgery: a case report, *J. Med. Case Rep.* 12 (2018) 136, <https://doi.org/10.1186/s13256-018-1671-6>.
- [22] D.J. Lubin, S.B. Holden, M.B. Rettig, R.E. Reiter, C.R. King, J.M. Lee, D.W. Wallace, J. Calais, Prostate Cancer Pulmonary Metastasis Presenting as a Ground-Glass Pulmonary Nodule on 68Ga-PSMA-11 PET/CT, *Clin. Nucl. Med.* 44 (2019) e353–e356, <https://doi.org/10.1097/RLU.0000000000002499>.
- [23] J.B. Seo, J.G. Im, J.M. Goo, M.J. Chung, M.Y. Kim, Atypical pulmonary metastases: spectrum of radiologic findings, *Radiographics* 21 (2001) 403–417.
- [24] L. Evangelista, A. Panunzio, E. Scagliori, P. Sartori, Ground glass pulmonary nodules: their significance in oncology patients and the role of computer tomography and 18F-fluorodeoxyglucose positron emission tomography, *Eur. J. Hybrid. Imaging* 2 (2018) 2, <https://doi.org/10.1186/s41824-017-0021-z>.